# The upregulation of lamin A/C as a compensatory mechanism during tight junction disruption in renal tubular cells mediated by calcium oxalate crystals

Sudarat Hadpech, Paleerath Peerapen, Visith Thongboonkerd [*]

*Medical Proteomics Unit, Research Department, Faculty of Medicine Siriraj Hospital, Mahidol University, Bangkok 10700, Thailand*

A B S T R A C T

Calcium oxalate monohydrate (COM), the most important crystal causing kidney stone disease, upregulates lamin A/C but downregulates zonula occludens-1 (ZO-1) in renal tubular cells. While roles for F-actin and α-tubulin and their association with ZO-1 are known to regulate COM-mediated tight junction (TJ) disruption, roles of lamin A/C and its interplay with ZO-1 in COM kidney stone model remain unclear and are thus the objectives of this study. Lamin A/C was knocked down in MDCK cells by silencing RNA specific for *LMNA* (siLMNA). Both wild-type (WT) and siLMNA cells were treated with COM for 48-h compared with the untreated (control) cells. Western blotting and immunofluorescence staining revealed upregulated lamin A/C and down-regulated ZO-1 in the COM-treated WT cells. siLMNA successfully reduced lamin A/C expression in both control and COM-treated cells. Nonetheless, siLMNA did not reverse the effect of COM on the decreases in ZO-1 and transepithelial resistance, but further reduced their levels in both control and COM-treated cells. Protein-protein interaction analysis demonstrated that two cytoskeletal proteins (actin and tubulin) served as the linkers to connect lamin A/C with ZO-1 and occludin (both of which are the TJ proteins). Altogether, these data implicate that lamin A/C and ZO-1 are indirectly associated to control TJ function, and ZO-1 expression is regulated by lamin A/C. Moreover, COM-induced upregulation of lamin A/C most likely serves as a compensatory mechanism to cope with the downregulation of ZO-1 during COM-mediated TJ disruption.

## Introduction

Kidney stone disease is one form of crystallopathies caused by mineral crystals that originate and grow inside the kidney and/or urinary tract. Calcium oxalate monohydrate (COM), the most important crystalline form causing kidney stone disease, acts as an external stimulus to trigger various cellular responses (Peerapen and Thongboonkerd, 2021b; Thongboonkerd, 2019). COM crystals can be internalized into renal tubular cells after adhesion to the cells (Chaiyarit et al., 2016; Kanlaya et al., 2013). This crystal-uptake process can induce reorganization of intermediate filament and accumulation of F-actin at the internalization site (Lieske et al., 1994). Our recent studies have revealed that COM mediates tight junction (TJ) disruption and downregulates TJ-associated protein (zonula occludens-1 or ZO-1) via F-actin reorganization and α-tubulin relocalization (Hadpech et al., 2022; Peerapen and Thongboonkerd, 2021a). Stabilization of F-actin and

α-tubulin by phalloidin and docetaxel, respectively, can prevent TJ disruption and ZO-1 downregulation (Hadpech et al., 2022; Peerapen and Thongboonkerd, 2021a).

In addition, our previous expression proteomics study has shown that COM upregulates cellular expression of lamin A/C (Semangoen et al., 2008). A functional study has revealed that knockdown of *LMNA* gene encoding lamin A/C can suppress expression of several COM crystal receptors on the cell membranes, thereby reducing crystal-cell adhesion (Pongsakul et al., 2016). Recent evidence has also shown that infectious and chemical stimuli cause changes in lamin A/C together with alterations in TJ complex and receptors on the cell membranes in endothelial cells (Karakaya et al., 2022; Wutti-mongkolchai et al., 2022), suggesting association among lamin A/C, TJ complex, and the cell membranes. While the roles for F-actin and α-tubulin and their association with ZO-1 are known to regulate COM-mediated TJ disruption (Hadpech et al., 2022; Peerapen and

---

* Corresponding author at: Head of Medical Proteomics Unit, Research Department, Siriraj Hospital, Mahidol University, 6th Floor - SiMR Building, 2 Wanglang Road, Bangkoknoi, Bangkok 10700, Thailand.

*E-mail addresses:* thongboonkerd@dr.com, vthongbo@yahoo.com (V. Thongboonkerd).

Thongboonkerd, 2021a), the role of lamin A/C in COM kidney stone model remains unclear. Based on our previous findings (Pongsakul et al., 2016; Semangoen et al., 2008) and recent studies (Karakaya et al., 2022; Wuttimongkolchai et al., 2022), we hypothesized that lamin A/C might be associated with ZO-1 and its upregulation might be related to the COM-induced TJ disruption (either as the cause or the effect). The present study, therefore, addressed the roles for lamin A/C and its association with ZO-1 in COM-mediated TJ disruption.

## Materials and methods

### Cell culture and polarization

High-passage parental Madin-Darby canine kidney cell line (MDCKII; ATCC CRL-2936) (ATCC; Manassas, VA) was maintained in a complete growth medium containing Dulbecco's Modified Eagle Medium (DMEM) (Gibco; Grand Island, NY) supplemented with 10 % fetal bovine serum (FBS) (Gibco), 60 U/ml penicillin G (Sigma-Aldrich; St. Louis, MO), and 60 µg/ml streptomycin (Sigma-Aldrich). The cells (at 3rd to 10th passage) were incubated in humidified incubator with 5 % $CO_2$ at 37 °C. To achieve polarization, the cells ($7.5 \times 10^4$ cells/well) were seeded onto collagen-coated polyethylene cell culture insert (0.4-µm-pore-size, 1.12-$cm^2$-area) in the 12-mm Transwell (Corning Costar; Cambridge, MA) and maintained in the complete growth medium for 96-h.

### Knockdown of lamin A/C by small-interfering RNA (siRNA)

Knockdown of *LMNA* gene encoding lamin A/C was performed according to the protocol previously described (Aluksanasuwan et al., 2017; Pongsakul et al., 2016) using siRNA harboring sequence specific to *LMNA* (siLMNA) (Santa Cruz Biotechnology; Santa Cruz, CA). In *Canis lupus familiaris*, this siLMNA specifically targets at the 822nd – 842nd nucleotides of lamin A pre-mRNA. Since lamin A mRNA and lamin C mRNA are the alternative splicing products of pre-lamin A mRNA and the target region of siLMNA exists in both of them, siLMNA should be able to knockdown both lamin A and lamin C (Fig. 1). The cells were cultured in DMEM with 10 % FBS without antibiotics in 6-well plate (Corning Costar) until 60–80 % confluent. siLMNA was premixed with siRNA Transfection Reagent (Santa Cruz Biotechnology) in Opti-MEM (Gibco) and incubated at 25 °C for 45 min. A total of 80 pmol of

siLMNA was then added and incubated with the cells in humidified incubator with 5 % $CO_2$ at 37 °C for 5-h. Thereafter, the cells were further incubated in the complete growth medium for 24-h followed by subsequent investigations.

### Preparation of COM crystals

COM crystals were generated using the protocol established previously (Thongboonkerd et al., 2008; Thongboonkerd et al., 2006). Briefly, 10 mM $CaCl_2 \cdot 2H_2O$ in a buffer containing 10 mM Tris-HCl and 90 mM NaCl (pH 7.4) was mixed 1:1 (v/v) with 1.0 mM $Na_2C_2O_4$ in the same buffer to make their final concentrations at 5 mM and 0.5 mM, respectively. The mixture was incubated at 25 °C overnight, and the COM crystals were harvested by a centrifugation at $2,000 \times g$ for 5 min. The crystals were washed three times with methanol and air-dried overnight at 25 °C. The typical morphology of COM crystal was confirmed under an inverted phase-contrast light microscope (Eclipse Ti-S) (Nikon; Tokyo, Japan). The crystals were decontaminated by UV light radiation for 30 min before exposure to the cells.

### COM treatment

Both wild-type (WT) and siLMNA-transfected MDCK cells were incubated with the sublethal concentration of COM (100 µg of COM crystal per 1 ml of culture medium) in humidified incubator with 5 % $CO_2$ at 37 °C for 48-h (Semangoen et al., 2008; Vinaiphat et al., 2017). Thereafter the cells were subjected to Western blot analysis and immunofluorescence study as follows.

### Western blot analysis

Western blotting was performed as described previously (Fong-ngern et al., 2017a; Fong-ngern et al., 2017b). Briefly, cellular proteins (30 µg/lane) were resolved by 12 % SDS-PAGE and transferred to a nitrocellulose membrane (EMD Millipore; Billerica, MA) using a semi-dry transfer unit (GE Healthcare; Uppsala, Sweden) at 85 mA for 1.5 h. After blocking non-specific binders with 5 % skim-milk/PBS for 1 h, the membrane was incubated overnight at 4 °C with mouse monoclonal anti-LMNA (Santa Cruz Biotechnology) (1:1,000), mouse monoclonal anti-ZO-1 (Invitrogen; Eugene, OR) (1:1,000), or mouse monoclonal



**siLMNA**
21-nucleotide-long, targeting at 822nd – 842nd nucleotides of lamin A pre-mRNA of *Canis lupus familiaris*
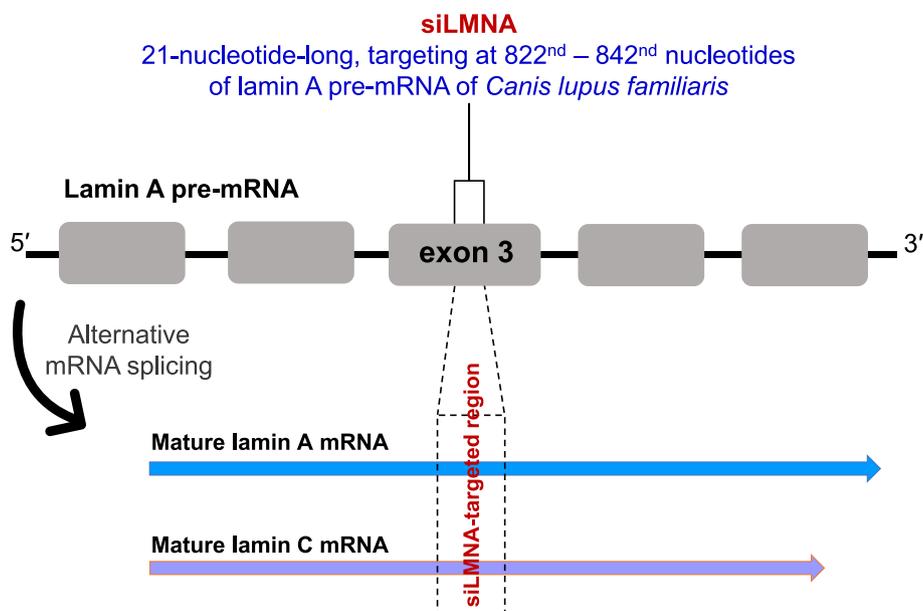
**Fig. 1.** siLMNA target. The target of siLMNA is at 822nd–842nd nucleotides within exon 3 of lamin A pre-mRNA of *Canis lupus familiaris*. Both lamin A and lamin C are derived from lamin A pre-mRNA by alternative splicing and share this siLMNA-targeted region.

anti-glyceraldehyde-3-phosphate dehydrogenase (GAPDH) (Santa Cruz Biotechnology) (1:2,000) antibody in 1 % skim milk/PBS. After three washes with PBS, the membrane was incubated with rabbit anti-mouse IgG conjugated with horseradish peroxidase (1:20,000 in 1 % skim-milk/PBS) (Sigma-Aldrich) at 25 °C for 1 h. Immunoreactive protein bands were visualized by SuperSignal West Pico chemiluminescence substrate (Pierce Biotechnology, Inc.; Rockford, IL) and quantified by using ImageQuant TL software (GE Healthcare).

*Immunofluorescence study*

Immunofluorescence stainings were performed using protocol reported previously (Vinaiphat and Thongboonkerd, 2018; Yoodee et al., 2021). Briefly, the cells were fixed with 4 % paraformaldehyde/PBS at 25 °C for 15 min, permeabilized with 0.1 % Triton X-100/PBS at 25 °C for 15 min, and then washed with membrane preserving buffer (PBS containing 0.1 mM CaCl$_2$ and 1 mM MgCl$_2$). The cells were incubated with 5 % bovine serum albumin (BSA)/PBS at 25 °C for 30 min to block non-specific binders and then with mouse monoclonal anti-LMNA (Santa Cruz Biotechnology) or mouse monoclonal anti-ZO-1 (Invitrogen) antibody (both at 1:50 in 1 % BSA/PBS) at 37 °C for 1 h. After three washes with PBS, the cells were incubated with goat anti-mouse IgG conjugated with Alexa Fluor 488 (green) (Invitrogen) (1:5,000) mixed with Hoechst dye (Invitrogen) (1:1,000) in 1 % BSA/PBS at 37 °C for 1 h. After extensive washes with PBS and mounting on a glass slide, the cells were examined and imaged under Eclipse 80i fluorescence microscope (Nikon). Quantitative intensity data were measured from at least 100 cells in $\geq$ 10 random high-power fields (HPFs) per each biological sample using NIS-Elements D V.4.11 (Nikon). Using this software, distribution of the immunofluorescence signal was analyzed in its spectral format to localize protein expression.

*Measurement of transepithelial resistance (TER)*

At 0, 12, 24, 36 and 48 h after COM exposure, TER was measured in the Transwell with polarized cell monolayer using Millicell-ERS resistance system (Millipore; Bedford, MA) as described previously (Sueksakit and Thongboonkerd, 2021; Vinaiphat et al., 2018). Measurements were performed at three different areas in each sample well. Background subtraction was done using the resistance obtained from the blank coated well filled with the complete growth medium but without cells. TER was then calculated using the following formula:

TER ($\Omega \cdot cm^2$) = (Resistance of sample well – Resistance of blank well) ($\Omega$) × Well area ($cm^2$).

*Protein-protein interaction analysis*

Lamin A/C (*LMNA*) was subjected to analysis for its interaction with TJ proteins known to get involved in COM-induced TJ disruption, including ZO-1 (*TJP1*) and occludin (*OCLN*) (Peerapen and Thongboonkerd, 2011, 2013). Such protein–protein interaction analysis was performed using the STRING tool (version 11.5) (*https://string-db.org*) by inputting the target protein (*LMNA*) together with candidates for the interaction (*TJP1* and *OCLN*). The protein–protein interaction was also openly queried through experimental/literature evidence and/or knowledge database retrieved by the STRING tool. Greater details can be found at *https://string-db.org*.

*Statistical analysis*

All quantitative data were obtained from three independent experiments using different biological samples (n = 3) and are presented as mean ± SEM. Comparisons between two groups were done using

unpaired Student's *t* test, whereas multiple comparisons were done using one-way analysis of variance (ANOVA) with Tukey's post-hoc test. *P* values < 0.05 were considered statistically significant.

## Results

*COM upregulated lamin A/C in renal tubular cells*

After 48-h incubation with or without COM, expression level of lamin A/C was examined by Western blot analysis and immunofluorescence study. Western blotting revealed that lamin A/C level was increased by COM treatment as compared with the untreated (control) cells (Fig. 2A-2C). Such increase of lamin A/C mediated by COM was confirmed by immunofluorescence study (Fig. 2D-2F).

*Effects of lamin A/C knockdown on downregulation and redistribution of ZO-1 mediated by COM*

From our previous studies, COM induces ZO-1 downregulation (Peerapen and Thongboonkerd, 2011, 2013, 2021a). By contrast, COM upregulates lamin A/C as shown in our previous report (Pongsakul et al., 2016) and herein (Fig. 2). To further investigate whether the COM-mediated decrease of ZO-1 is related to or regulated by the upregulated lamin A/C, MDCK cells with *LMNA* gene knockdown were constructed by siRNA technique. Western blot analysis revealed that siRNA targeting the *LMNA* gene (siLMNA) successfully reduced lamin A/C expression to approximately 1/2 of its basal level in the WT cells (Fig. 3). Also, siLMNA could prevent the COM-mediated increase in lamin A/C as compared with the untreated (control) siLMNA-transfected cells.

As expected, ZO-1 level was dramatically decreased by COM in the WT cells (Fig. 3). However, *LMNA* gene knockdown did not prevent such COM-mediated decrease in ZO-1 level in the siLMNA-transfected cells. It appeared that *LMNA* gene knockdown further downregulated the ZO-1 expression in both untreated (control) and COM-treated siLMNA-transfected cells to lower than a half (Fig. 3).

Similar to the data obtained from Western blotting, immunofluorescence study revealed that lamin A/C expression at nuclei was increased by COM treatment in the WT cells (Fig. 4A-4D). siLMNA could prevent the COM-mediated increase in lamin A/C as compared with the untreated (control) siLMNA-transfected cells. By contrast, ZO-1 level was dramatically reduced by COM treatment in the WT cells (Fig. 4E-4H). ZO-1 expression at cell borders was distorted by COM, while its redistribution to cytoplasm and nuclei was also observed (Fig. 4E and 4F). Moreover, *LMNA* gene knockdown did not prevent but worsened such COM-mediated decrease in ZO-1 level in the siLMNA-transfected cells (Fig. 4E-4H).

*Effects of lamin A/C knockdown on TJ disruption mediated by COM*

Our previous studies have clearly demonstrated that COM causes TJ disruption (Peerapen and Thongboonkerd, 2011, 2013, 2021a). To further investigate whether the COM-mediated TJ disruption is regulated by lamin A/C, transepithelial resistance (TER), which reflects TJ barrier function, was examined. As expected, the data clearly showed that TER was obviously reduced by COM treatment in the WT cells at all time-points (Fig. 5). In consistent with the data on ZO-1 expression, *LMNA* gene knockdown further reduced TER in both untreated (control) and COM-treated siLMNA-transfected cells (Fig. 5).

*Interplay among lamin A/C, TJ proteins, and cytoskeletal proteins*

To analyze the interplay among lamin A/C, TJ proteins, and cytoskeletal proteins, protein–protein interaction was analyzed by using the STRING analysis tool. Lamin A/C (*LMNA*) was subjected to analysis for its association with TJ proteins known to get involved in COM-induced TJ disruption, including ZO-1 (*TJP1*) and occludin (*OCLN*) (Peerapen
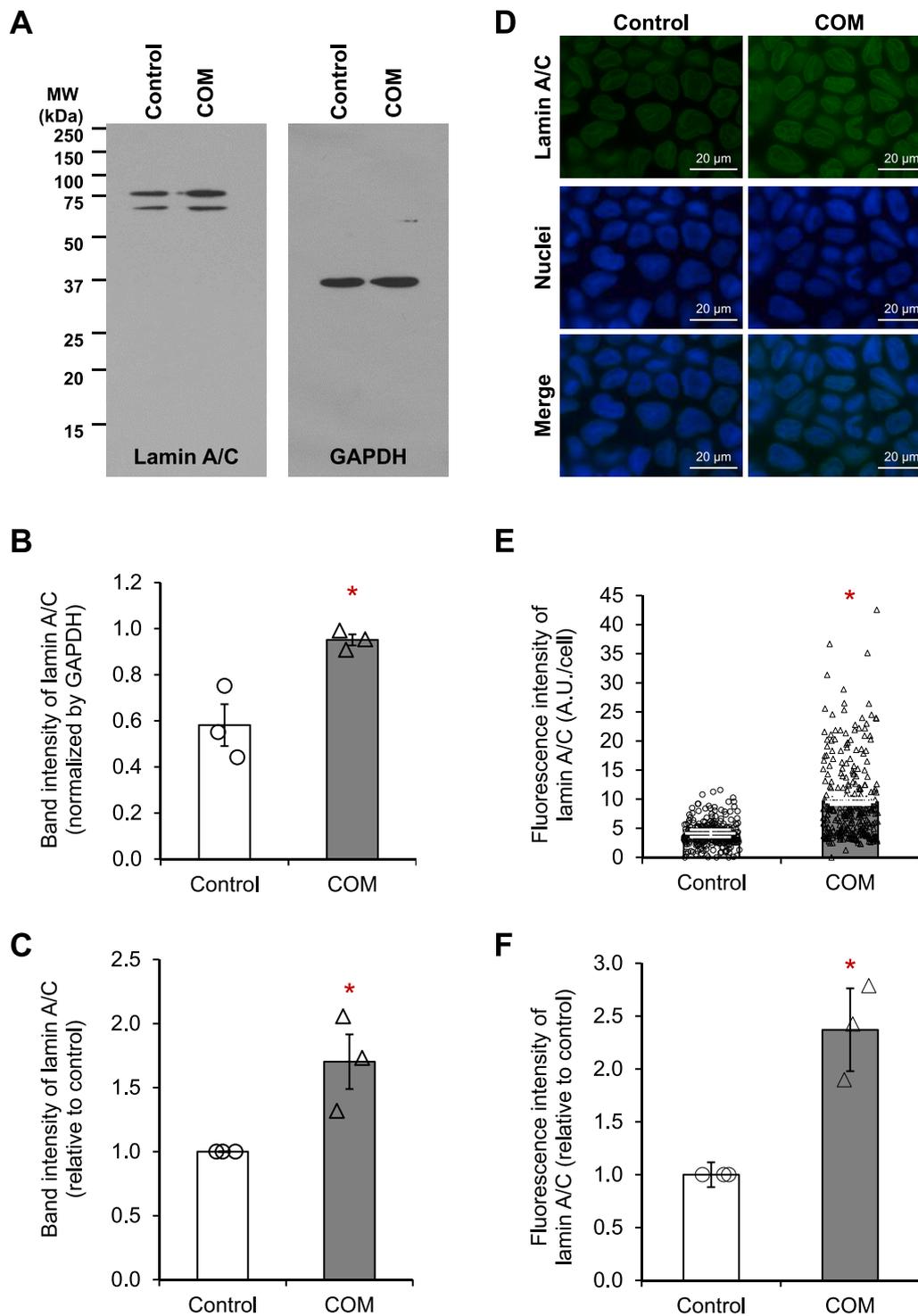
**Fig. 2.** COM upregulated lamin A/C in renal tubular cells. After polarization followed by 48-h incubation with or without COM crystals, level of lamin A/C in MDCK cells was examined. (A): Western blot analysis of lamin A/C using GAPDH as a loading control. (B) and (C): Band intensity of lamin A/C was quantified by using ImageQuant TL software (GE Healthcare) and was relative to GAPDH and control group, respectively. (D): Immunofluorescence staining of lamin A/C (green) and nuclei (blue). (E): Fluorescence intensity data were measured from 100 cells in ≥ 10 random high-power fields per each biological sample. (F): The fluorescence intensity data were relative to the control group. Each bar represents mean ± SEM of the data derived from three independent experiments using different biological samples (n = 3) (A.U. = arbitrary unit). * = p < 0.05 vs. control. (For interpretation of the references to colour in this figure legend, the reader is referred to the web version of this article.)

and Thongboonkerd, 2011, 2013). The analysis was also openly queried through experimental evidence and/or knowledge database (*https://string-db.org*). The data showed that lamin A/C was directly associated with two cellular cytoskeletal proteins, including actin (*ACTB*) and tubulin α-1 chain (*TUBA1A*) (Fig. 6). Additionally, these two

cytoskeletal proteins further connected to both TJ proteins, ZO-1 (*TJP1*) and occludin (*OCLN*). Although protein–protein interaction analysis did not show a direct association between lamin A/C and ZO-1, this result implicated their indirect interplay via actin (*ACTB*) and tubulin α-1 chain (*TUBA1A*), which served as the linkers between nuclear lamin A/C
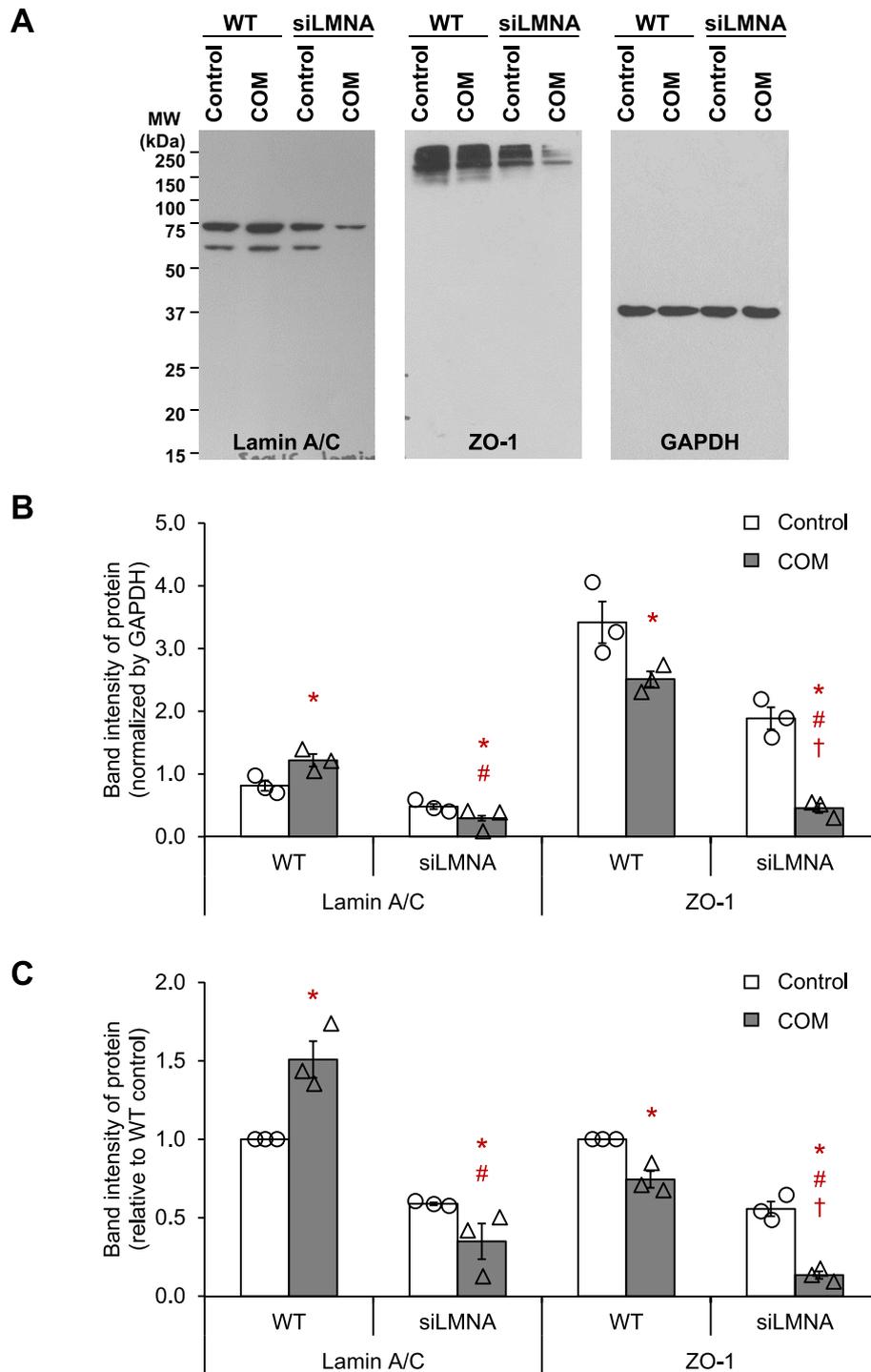
**Fig. 3.** Levels of lamin A/C and ZO-1 in wild-type (WT) and siLMNA-transfected MDCK cells with or without COM treatment. After polarization followed by 48-h incubation with or without COM crystals, levels of lamin A/C and ZO-1 in WT and siLMNA-transfected MDCK cells were examined. (A): Western blot analysis of lamin A/C and ZO-1 using GAPDH as a loading control. (B) and (C): Band intensity of each protein was quantified by using ImageQuant TL software (GE Healthcare) and was relative to GAPDH and WT control group, respectively. Each bar represents mean ± SEM of the data derived from three independent experiments using different biological samples (n = 3). * = p < 0.05 vs. control WT cells; # = p < 0.05 vs. COM-treated WT cells; † = p < 0.05 vs. control siLMNA-transfected cells.

and TJ proteins (Fig. 6).

## Discussion

Cells are frequently exposed to various types of external stimuli causing different cellular responses (Humphrey et al., 2014). The cell plasma membranes serve as the primary site for receiving signal loads and then transmit and translate them through a pathway called mechanotransduction (Martino et al., 2018; Uray and Uray, 2021). Various cellular components, including membrane receptors (e.g., integrin), linker proteins (e.g., talin and vinculin), cytoskeletal proteins (e.g., F-actin, microtubules and intermediate filaments), and nuclear lamina proteins (lamin A/C and lamin B) are known to play essential roles in the mechanosignaling pathway (Humphrey et al., 2014;
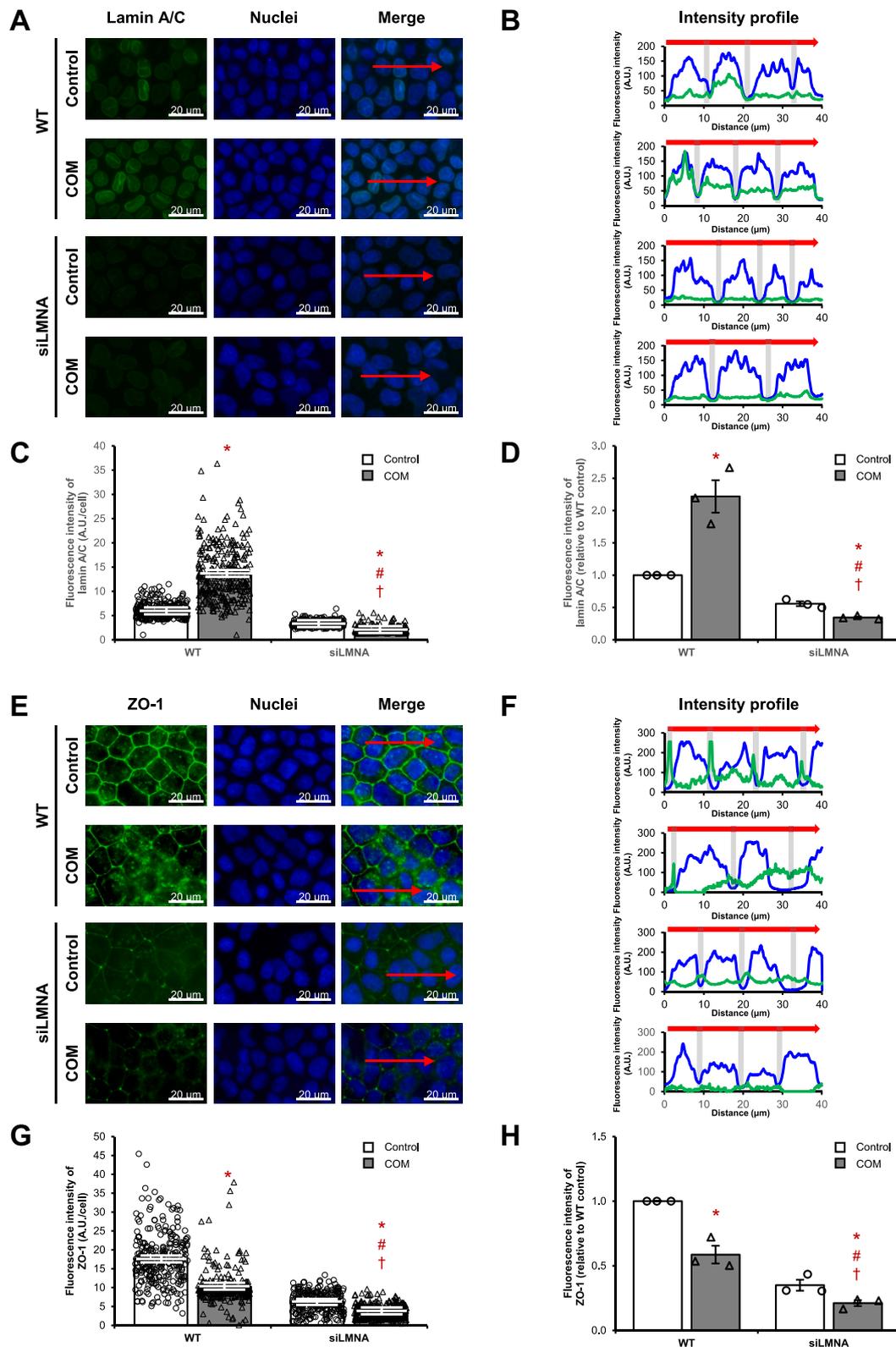
**Fig. 4.** Effects of lamin A/C knockdown on downregulation and redistribution of ZO-1 mediated by COM. After polarization followed by 48-h incubation with or without COM crystals, levels of lamin A/C and ZO-1 in wild-type (WT) and siLMNA-transfected MDCK cells were examined. (A) and (E): Both lamin A/C and ZO-1 are shown in green, whereas nuclei are shown in blue. (B) and (F): Their spectral patterns of the immunofluorescence signals across the cells are also shown. The area of spectral data plot is localized by the horizontal red arrow, whereas the cell border is indicated by the vertical gray bar. (C) and (G): Quantitative fluorescence intensity data were measured from 100 cells in ≥ 10 random high-power fields per each biological sample. (D) and (H): The fluorescence intensity data were relative to the WT control group. Each bar represents mean ± SEM of the data derived from three independent experiments using different biological samples (n = 3) (A.U. = arbitrary unit). * = p < 0.05 vs. control WT cells; # = p < 0.05 vs. COM-treated WT cells; † = p < 0.05 vs. control siLMNA-transfected cells. (For interpretation of the references to colour in this figure legend, the reader is referred to the web version of this article.)
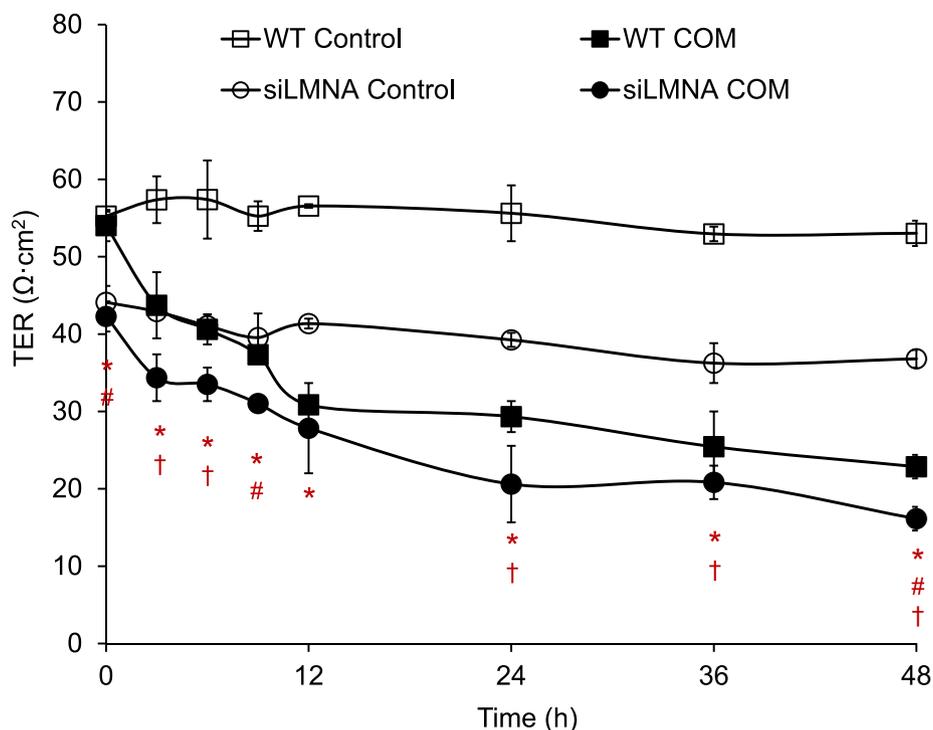
**Fig. 5.** Effects of lamin A/C knockdown on TJ disruption mediated by COM. After polarization followed by 48-h incubation with or without COM crystals, trans-epithelial resistance (TER) levels in wild-type (WT) and siLMNA-transfected MDCK cells were examined. TER measurements were performed at three different areas in each sample well. Background subtraction was done using the resistance obtained from the blank coated-well filled with the complete growth medium but without cells. Each data point represents mean ± SEM of the measurements derived from three independent experiments using different biological samples (n = 3). * = p < 0.05 vs. control WT cells; # = p < 0.05 vs. COM-treated WT cells; † = p < 0.05 vs. control siLMNA-transfected cells.
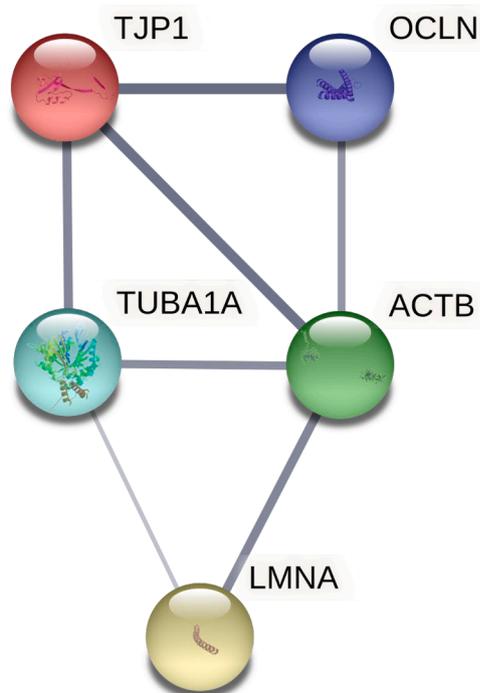


**Fig. 6.** Interplay among lamin A/C, TJ proteins, and cytoskeletal proteins. The interplay of lamin A/C (*LMNA*) with the TJ proteins known to get involved in COM-induced TJ disruption, including ZO-1 (*TJP1*) and occludin (*OCLN*), was analyzed by using the STRING tool (version 11.5) (*https://string-db.org*). The protein–protein interaction was also openly queried through experimental evidence and/or knowledge database. *ACTB* encodes actin and *TUBA1A* encodes tubulin α-1 chain.

Osmanagic-Myers et al., 2015; Uray and Uray, 2021).

Lamins are members of type V intermediate filaments (de Leeuw et al., 2018). They play several essential roles in nuclear structure stabilization, chromosome organization, and gene transcription/regulation (de Leeuw et al., 2018; Dubik and Mai, 2020). Lamin A/C is an A-type lamin protein that localizes in nuclear lamina between the nuclear envelope and chromatin (Dubik and Mai, 2020; Vahabikashi et al., 2022). It binds to B-type lamin and other associated proteins to form a meshwork under the inner nuclear membrane (Malashicheva and Perepelina, 2021; Turgay et al., 2017; Turgay and Medalia, 2017; Vahabikashi et al., 2022). Lamin A/C also serves as a mechanosensor to receive signals from external stimuli and to trigger internal biological processes (Osmanagic-Myers et al., 2015; Vahabikashi et al., 2022). For example, external shear force can upregulate expression of lamin A/C and translocate it from intranuclear locale to the perinuclear site, where lamin A/C can regulate nuclear shape and gene expression in aging model (Philip and Dahl, 2008). With its multifaceted roles, lamin A/C requires many binding or interacting proteins to support its functions (Malashicheva and Perepelina, 2021). For example, it interacts with cellular cytoskeletal complex, including F-actin, microtubule and intermediate filament, to maintain nuclear structure and function (Antmen et al., 2021; Chatzifrangkeskou et al., 2023; Malashicheva and Perepelina, 2021; Tariq et al., 2017; Wang et al., 2023).

Our present study revealed that COM induced renal tubular cell responses by upregulating lamin A/C and downregulating ZO-1. To address the association between lamin A/C upregulation and ZO-1 downregulation, *LMNA* gene knockdown was performed. Our data demonstrated that *LMNA* gene knockdown did not reverse the effects of COM on the decreases of ZO-1 and TER levels. Furthermore, *LMNA* gene knockdown worsened the COM-mediated decreases of ZO-1 and TER levels. Therefore, COM-induced lamin A/C upregulation is unlikely to be the causative or pathogenic mechanism underlying the COM-mediated TJ disruption (otherwise, *LMNA* gene knockdown should be able to

rescue the COM-mediated effects on ZO-1 and TER). But our study has shown the opposite data. Hence, the COM-induced lamin A/C upregulation most likely serves as a compensatory mechanism to cope with the COM-mediated ZO-1 downregulation and TJ disruption (Fig. 7).

In our study model, COM serves as an external stimulus to induce cellular responses. As COM has a potent adhesive force to adhere tightly with renal tubular cells (Peerapen and Thongboonkerd, 2020), one of the possible cellular responses is to trigger the mechanosensing pathway to cope with the COM-induced deteriorations (particularly TJ

disruption) via the upregulation of lamin A/C as the compensatory mechanism. Our hypothesis is supported by a recent study demonstrating that lamin A/C overexpression or upregulation is a repairing mechanism to cope with minor rotator cuff injury (Gumina et al., 2021). However, when the rotator cuff gets extensive tears beyond the compensatory mechanism, lamin A/C, on the other hand, is downregulated (Gumina et al., 2021). This may also explain the phenomenon observed in our present study regarding the downregulation of lamin A/C in the siLMNA-transfected cells treated with COM crystals
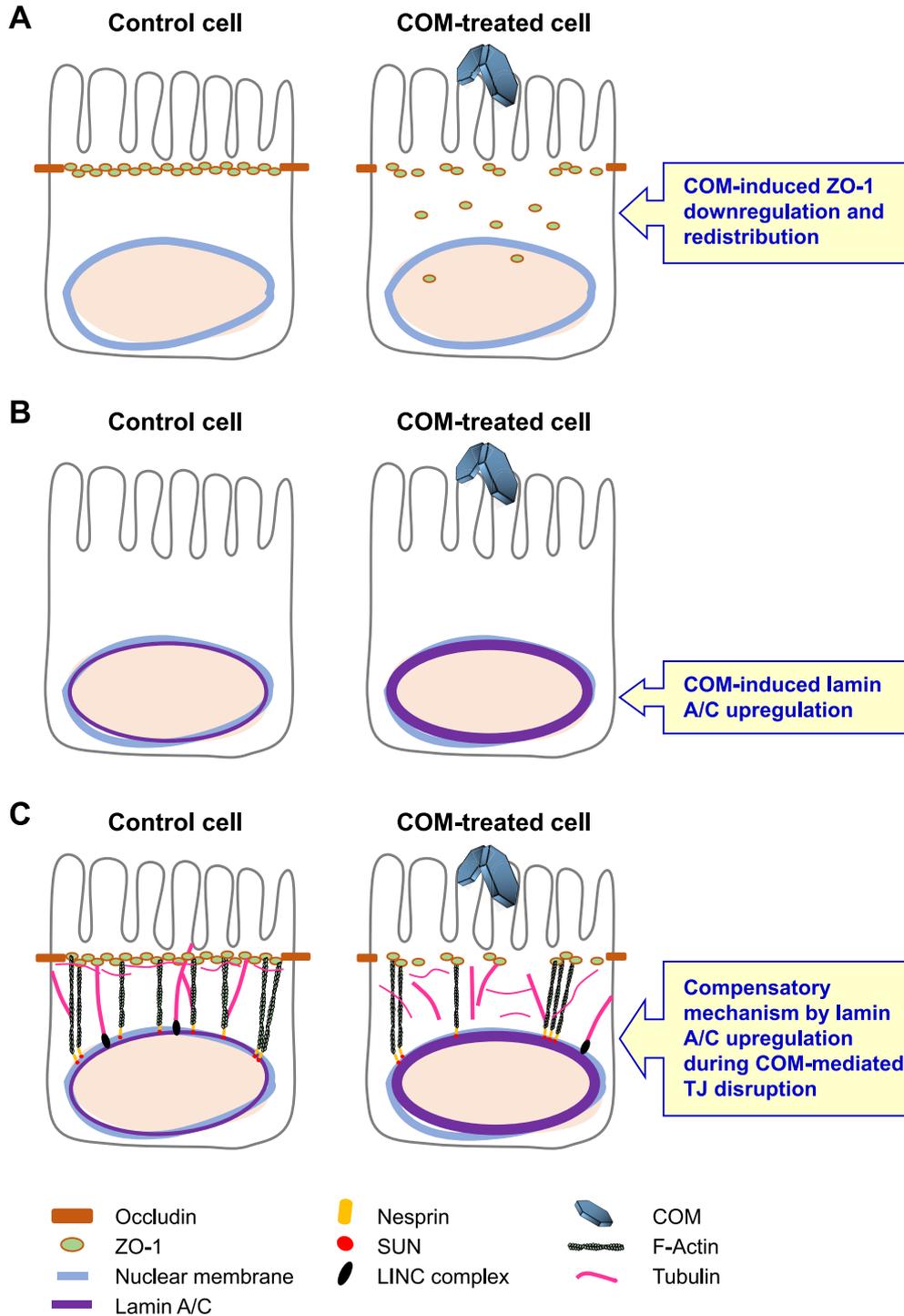


**Fig. 7.** Summary of the effects of COM on ZO-1 and lamin A/C in renal tubular cells. (A): COM-induced ZO-1 downregulation/redistribution. (B): COM-induced lamin A/C upregulation. (C): Merged image of (A) and (B) with changes in cytoskeletal assembly to summarize compensatory mechanism by lamin A/C upregulation during COM-mediated TJ disruption. SUN = Sad1 and UNC84 homology. LINC = the linker of nucleoskeleton and cytoskeleton.

(representing the severe stress that is beyond the compensatory mechanism), whereas lamin A/C is upregulated in the COM-treated WT cells (representing the mild stress condition) (Figs. 3 and 4). Nevertheless, the precise mechanosensing-related mechanism in kidney stone model triggered by COM remains to be elucidated with further investigations.

As COM is known to induce cellular responses via cytoskeletal network and affects the cellular junctional complex (Peerapen et al., 2018; Peerapen and Thongboonkerd, 2021a), it is thus plausible that lamin A/C is not associated with ZO-1 directly, but depends on other proteins that serve as the linkers between both of them. We further investigated whether there is an indirect association between these two proteins via linkers or other associated proteins using the STRING analysis tool. The data derived from the STRING prediction implicate that lamin A/C is directly associated with actin and α-tubulin, but is indirectly associated with ZO-1 and occludin, which are members of the TJ protein complex. This protein network analysis has demonstrated the interplay of cytoskeletal proteins linking the nuclear lamina to the TJ protein complex. These data are consistent with those reported previously indicating that the cytoskeleton and nucleoskeleton are connected and coordinated functionally (Herlitz et al., 2012; Tariq et al., 2017; Uray and Uray, 2021).

Our data have also shown that COM causes not only ZO-1 downregulation but also its redistribution from the cell borders to cytoplasm and nuclei. Because renal tubular cells have a renewal capability, which normally occurs after cell injury (Fujigaki, 2012), it may be possible that ZO-1 redistribution is related to a regeneration process following COM-induced cellular injury. This hypothesis is supported by a study that describes ZO-1 redistribution in an early phase of physiologic cell shedding during intestinal cellular renewal process (Guan et al., 2011). Consistently, a recent study has shown that the distribution/localization of ZO-1 can be altered during cell turnover or proliferation (Imafuku et al., 2023). Other independent studies have revealed that ZO-1 can be localized in the nuclei and can regulate gene expression (Balda et al., 2003; Balda and Matter, 2000; Zhong et al., 2012). Therefore, another possibility is that the COM-induced ZO-1 redistribution is to regulate gene expression during the COM-mediated TJ disruption.

In addition to the role in sensing mechanical forces from external stimuli (de Leeuw et al., 2018; Lammerding et al., 2004; Vahabikashi et al., 2022), another important role of lamin A/C is to stabilize nuclear structure (Dubik and Mai, 2020; Vahabikashi et al., 2022). In *LMNA*$^{-/-}$ mouse fibroblasts, the cells have impaired nuclear mechanics associated with increased nuclear fragility and reduced cytoskeletal stiffness (Lammerding et al., 2004). In consistent, actin polymerization and organization are disturbed in *LMNA*$^{-/-}$ and *LMNA*-mutated N195K cells (Ho et al., 2013). Moreover, *LMNA*$^{-/-}$ mouse embryonic fibroblasts have impaired actin fiber organization and less cytoskeletal components (van Loosdregt et al., 2017). Additionally, these *LMNA*-knockout fibroblasts exhibit less contractile property as compared with the WT fibroblasts (van Loosdregt et al., 2017). In the present study, we found that the siLMNA-transfected renal tubular cells had lower TER than the WT cells even without induction by COM. This result implies that the siLMNA-knockdown cells have less cellular integrity than the WT cells as the data clearly showed further reduction of TER when the effect of *LMNA* gene knockdown was combined with the effect of COM. These data were consistent with the loss of ZO-1 level in the former experiment implicating that lamin A/C is one of the key proteins involved in COM responses to regulate TJ protein complex via cytoskeletal network complex.

Structurally, the linker of nucleoskeleton and cytoskeleton (LINC) complex crosses the nuclear envelope, thereby connecting the cytoplasmic compartment to the nucleus (Gurusaran and Davies, 2021). The LINC complex consists of (i) SUN (Sad1 and UNC84 homology) domain and (ii) KASH (Klarsicht, ANC-1, and Syne homology) domain. SUN directly binds to lamin A/C, whereas KASH interacts with actin filament via nesprin 1/2, binds to microtubule via kinesin and dynein motor, and binds to intermediate filament via nesprin 3 (Gurusaran and Davies,

2021; Malashicheva and Perepelina, 2021). Microtubule is associated with ZO-1 (Jalimarada et al., 2009; Thanuja et al., 2021), occludin (Glotfelty et al., 2014), and actin via microtubule-actin crosslinking factor (MACF) (Sun et al., 2001). Our previous study has also reported that tubulin (a microtubular protein), vimentin (an intermediate filament protein), S100, α-enolase, and annexin A2 are associated with lamin A/C, and knockdown of the *LMNA* gene can reduce their expression levels (Pongsakul et al., 2016). Herein, we observed that *LMNA* gene knockdown also downregulated ZO-1 expression, implying that TJ disruption in the siLMNA-transfected cells is caused by lamin A/C-dependent ZO-1 expression regulation. ZO-1 is an adaptor protein that plays role in the formation, maintenance and regulation of TJ. Alongside claudin and occludin, ZO-1 supports the TJ structure and links the TJ complex to intracellular cytoskeletal assembly (Odenwald et al., 2018; Otani et al., 2019). This intricate network further strengthens the TJ function as the paracellular barrier to control the passage of molecules across epithelial layer and participates in intracellular signaling cascades (Itoh et al., 2018; Rouaud et al., 2020).

Although the data reported herein are promising and may partially explain some biological phenomena during the COM-mediated TJ disruption, a number of limitations in our present study should be noted. First, the data were obtained solely from *in vitro* experiments, which might not entirely resemble the *in vivo* biological phenomena. Confirming these effects by *in vivo* study would strengthen our findings and conclusions. Second, the interplay among lamin A/C, TJ proteins and cytoskeletal proteins was analyzed only by bioinformatic prediction. Validation (e.g., by co-immunoprecipitation, tandem affinity purification, or other protein–protein interaction experiments) should be performed to strengthen such data on protein–protein interaction. Although we have not provided experimental data of lamin A/C and F-actin interaction, a previous study has demonstrated that lamin A/C requires the LINC complex to connect with the pool of F-actin in the cytoplasm (Vahabikashi et al., 2022). Another study has also demonstrated that F-actin binds directly to both lamin A and lamin B via actin-binding site-1 (Simon et al., 2010). They have further reported that actin-binding site-2 is specific for lamin A (Simon et al., 2010). Third, only ZO-1 and TER were examined in this study. In fact, there are several other TJ proteins that play crucial roles in maintaining TJ functions. Therefore, examining other TJ proteins and functions would gain more insights into the COM-induced TJ disruption. Finally, our data have led to the hypothesis that the upregulation of lamin A/C by COM is a potential compensatory mechanism to cope with the downregulated ZO-1 and TJ disruption mediated by COM. *LMNA* gene overexpression may be required to confirm this hypothesis by examining whether *LMNA* gene overexpression can prevent or lessen TJ disruption mediated by COM.

## Conclusions

We have reported herein that COM increases lamin A/C expression, decreases ZO-1 expression, and induces TJ disruption. Knockdown of *LMNA* gene does not prevent such COM-mediated decreases in ZO-1 and TER levels in the siLMNA-transfected cells. On the other hand, *LMNA* gene knockdown further downregulates ZO-1 expression and reduces TER in both untreated (control) and COM-treated siLMNA-transfected cells. Protein-protein interaction analysis reveals that lamin A/C is directly associated with two cellular cytoskeletal proteins, including actin and α-tubulin, which further connect to both TJ proteins, ZO-1 and occludin. Taken together, these data implicate that lamin A/C and ZO-1 are indirectly associated to control TJ function, and ZO-1 expression is regulated by lamin A/C. Moreover, COM-induced upregulation of lamin A/C most likely serves as a compensatory mechanism to cope with the downregulation of ZO-1 during COM-mediated TJ disruption (Fig. 7).

## CRediT authorship contribution statement

**Sudarat Hadpech:** Conceptualization, Methodology, Validation,

Formal analysis, Investigation, Data curation, Writing – original draft, Visualization. **Paleerath Peerapen:** Conceptualization, Methodology, Validation, Formal analysis, Investigation, Data curation, Visualization. **Visith Thongboonkerd:** Conceptualization, Methodology, Software, Validation, Resources, Writing – review & editing, Supervision, Funding acquisition.

## Declaration of competing interest

The authors declare that they have no known competing financial interests or personal relationships that could have appeared to influence the work reported in this paper.

## Data availability

Data will be made available on request.

## Acknowledgements

## References

Aluksanasuwan, S., Sueksakit, K., Fong-ngern, K., Thongboonkerd, V., 2017. Role of HSP60 (HSPD1) in diabetes-induced renal tubular dysfunction: regulation of intracellular protein aggregation, ATP production, and oxidative stress. FASEB J. 31, 2157–2167.

Antmen, E., Demirci, U., Hasirci, V., 2021. Micropatterned Surfaces Expose the Coupling between Actin Cytoskeleton-Lamin/Nesprin and Nuclear Deformability of Breast Cancer Cells with Different Malignancies. Adv. Biol. (weinh) 5, e2000048.

Balda, M.S., Garrett, M.D., Matter, K., 2003. The ZO-1-associated Y-box factor ZONAB regulates epithelial cell proliferation and cell density. J. Cell Biol. 160, 423–432.

Balda, M.S., Matter, K., 2000. The tight junction protein ZO-1 and an interacting transcription factor regulate ErbB-2 expression. EMBO J. 19, 2024–2033.

Chaiyarit, S., Singhto, N., Thongboonkerd, V., 2016. Calcium oxalate monohydrate crystals internalized into renal tubular cells are degraded and dissolved by endolysosomes. Chem. Biol. Interact. 246, 30–35.

Chatzifrangeskou, M., Le Dour, C., Muchir, A., 2023. Modulation of cytoskeleton in cardiomyopathy caused by mutations in LMNA gene. Am. J. Physiol. Cell Physiol. 324, C1223–C1235.

de Leeuw, R., Gruenbaum, Y., Medalia, O., 2018. Nuclear Lamins: Thin Filaments with Major Functions. Trends Cell Biol. 28, 34–45.

Dubik, N., Mai, S., 2020. Lamin A/C: Function in Normal and Tumor Cells. Cancers (basel) 12, 3688.

Fong-ngern, K., Ausakunpipat, N., Singhto, N., Sueksakit, K., Thongboonkerd, V., 2017a. Prolonged K(+) deficiency increases intracellular ATP, cell cycle arrest and cell death in renal tubular cells. Metabolism 74, 47–61.

Fong-ngern, K., Vinaiphat, A., Thongboonkerd, V., 2017b. Microvillar injury in renal tubular epithelial cells induced by calcium oxalate crystal and the protective role of epigallocatechin-3-gallate. FASEB J. 31, 120–131.

Fujigaki, Y., 2012. Different modes of renal proximal tubule regeneration in health and disease. World J. Nephrol. 1, 92–99.

Glotfelty, L.G., Zahs, A., Iancu, C., Shen, L., Hecht, G.A., 2014. Microtubules are required for efficient epithelial tight junction homeostasis and restoration. Am. J. Physiol. Cell Physiol. 307, C245–C254.

Guan, Y., Watson, A.J., Marchiando, A.M., Bradford, E., Shen, L., Turner, J.R., Montrose, M.H., 2011. Redistribution of the tight junction protein ZO-1 during physiological shedding of mouse intestinal epithelial cells. Am. J. Physiol. Cell Physiol. 300, C1404–C1414.

Gumina, S., Peruzzi, B., Leopizzi, M., Porta, N., Di Maio, V., Rocca, C.D., Candela, V., 2021. Nuclear lamin A in rotator cuff tear margin tenocytes: an antiapoptotic and cell mechanostat factor. J. Orthop. Surg. Res. 16, 413.

Gurusaran, M., Davies, O.R., 2021. A molecular mechanism for LINC complex branching by structurally diverse SUN-KASH 6:6 assemblies. Elife 10, e60175.

Hadpech, S., Peerapen, P., Thongboonkerd, V., 2022. Alpha-tubulin relocalization is involved in calcium oxalate-induced tight junction disruption in renal epithelial cells. Chem. Biol. Interact. 368, 110236.

Herlitz, L.C., D'Agati, V.D., Markowitz, G.S., 2012. Crystalline nephropathies. Arch. Pathol. Lab. Med. 136, 713–720.

Ho, C.Y., Jaalouk, D.E., Vartiainen, M.K., Lammerding, J., 2013. Lamin A/C and emerin regulate MKL1-SRF activity by modulating actin dynamics. Nature 497, 507–511.

Humphrey, J.D., Dufresne, E.R., Schwartz, M.A., 2014. Mechanotransduction and extracellular matrix homeostasis. Nat. Rev. Mol. Cell Biol. 15, 802–812.

Imafuku, K., Iwata, H., Natsuga, K., Okumura, M., Kobayashi, Y., Kitahata, H., Kubo, A., Nagayama, M., Ujiie, H., 2023. Zonula occludens-1 distribution and barrier functions are affected by epithelial proliferation and turnover rates. Cell Prolif. e13441.

Itoh, M., Nakadate, K., Matsusaka, T., Hunziker, W., Sugimoto, H., 2018. Effects of the differential expression of ZO-1 and ZO-2 on podocyte structure and function. Genes Cells 23, 546–556.

Jalimarada, S.S., Shivanna, M., Kini, V., Mehta, D., Srinivas, S.P., 2009. Microtubule disassembly breaks down the barrier integrity of corneal endothelium. Exp. Eye Res. 89, 333–343.

Kanlaya, R., Sintiprungrat, K., Chaiyarit, S., Thongboonkerd, V., 2013. Macropinocytosis is the major mechanism for endocytosis of calcium oxalate crystals into renal tubular cells. Cell Biochem. Biophys. 67, 1171–1179.

Karakaya, E., Abdul, Y., Chowdhury, N., Wellslager, B., Jamil, S., Albayram, O., Yilmaz, O., Ergul, A., 2022. Porphyromonas gingivalis infection upregulates the endothelin (ET) system in brain microvascular endothelial cells. Can. J. Physiol. Pharmacol. 100, 679–688.

Lammerding, J., Schulze, P.C., Takahashi, T., Kozlov, S., Sullivan, T., Kamm, R.D., Stewart, C.L., Lee, R.T., 2004. Lamin A/C deficiency causes defective nuclear mechanics and mechanotransduction. J. Clin. Invest. 113, 370–378.

Lieske, J.C., Swift, H., Martin, T., Patterson, B., Toback, F.G., 1994. Renal epithelial cells rapidly bind and internalize calcium oxalate monohydrate crystals. PNAS 91, 6987–6991.

Malashicheva, A., Perepelina, K., 2021. Diversity of Nuclear Lamin A/C Action as a Key to Tissue-Specific Regulation of Cellular Identity in Health and Disease. Front. Cell Dev. Biol. 9, 761469.

Martino, F., Perestrelo, A.R., Vinarsky, V., Pagliari, S., Forte, G., 2018. Cellular Mechanotransduction: From Tension to Function. Front. Physiol. 9, 824.

Odenwald, M.A., Choi, W., Kuo, W.T., Singh, G., Sailer, A., Wang, Y., Shen, L., Fanning, A.S., Turner, J.R., 2018. The scaffolding protein ZO-1 coordinates actomyosin and epithelial apical specializations in vitro and in vivo. J. Biol. Chem. 293, 17317–17335.

Osmanagic-Myers, S., Dechat, T., Foisner, R., 2015. Lamins at the crossroads of mechanosignaling. Genes Dev. 29, 225–237.

Otani, T., Nguyen, T.P., Tokuda, S., Sugihara, K., Sugawara, T., Furuse, K., Miura, T., Ebnet, K., Furuse, M., 2019. Claudins and JAM-A coordinately regulate tight junction formation and epithelial polarity. J. Cell Biol. 218, 3372–3396.

Peerapen, P., Chaiyarit, S., Thongboonkerd, V., 2018. Protein Network Analysis and Functional Studies of Calcium Oxalate Crystal-Induced Cytotoxicity in Renal Tubular Epithelial Cells. Proteomics 18, e1800008.

Peerapen, P., Thongboonkerd, V., 2011. Effects of calcium oxalate monohydrate crystals on expression and function of tight junction of renal tubular epithelial cells. Lab. Invest. 91, 97–105.

Peerapen, P., Thongboonkerd, V., 2013. p38 MAPK mediates calcium oxalate crystal-induced tight junction disruption in distal renal tubular epithelial cells. Sci. Rep. 3, 1041.

Peerapen, P., Thongboonkerd, V., 2020. Differential bound proteins and adhesive capabilities of calcium oxalate monohydrate crystals with various sizes. Int. J. Biol. Macromol. 163, 2210–2223.

Peerapen, P., Thongboonkerd, V., 2021a. Calcium oxalate monohydrate crystal disrupts tight junction via F-actin reorganization. Chem. Biol. Interact. 345, 109557.

Peerapen, P., Thongboonkerd, V., 2021b. Kidney stone proteomics: an update and perspectives. Expert Rev. Proteomics 18, 557–569.

Philip, J.T., Dahl, K.N., 2008. Nuclear mechanotransduction: response of the lamina to extracellular stress with implications in aging. J. Biomech. 41, 3164–3170.

Pongsakul, N., Vinaiphat, A., Chanchaem, P., Fong-ngern, K., Thongboonkerd, V., 2016. Lamin A/C in renal tubular cells is important for tissue repair, cell proliferation, and calcium oxalate crystal adhesion, and is associated with potential crystal receptors. FASEB J. 30, 3368–3377.

Rouaud, F., Sluysmans, S., Flinois, A., Shah, J., Vasileva, E., Citi, S., 2020. Scaffolding proteins of vertebrate apical junctions: structure, functions and biophysics. Biochim. Biophys. Acta Biomembr. 1862, 183399.

Semangoen, T., Sinchaikul, S., Chen, S.T., Thongboonkerd, V., 2008. Proteomic analysis of altered proteins in distal renal tubular cells in response to calcium oxalate monohydrate crystal adhesion: Implications for kidney stone disease. Proteomics Clin. Appl. 2, 1099–1109.

Simon, D.N., Zastrow, M.S., Wilson, K.L., 2010. Direct actin binding to A- and B-type lamin tails and actin filament bundling by the lamin A tail. Nucleus 1, 264–272.

Sueksakit, K., Thongboonkerd, V., 2021. Optimization of artificial urine formula for in vitro cellular study compared with native urine. Int. J. Med. Sci. 18, 3271–3279.

Sun, D., Leung, C.L., Liem, R.K., 2001. Characterization of the microtubule binding domain of microtubule actin crosslinking factor (MACF): identification of a novel group of microtubule associated proteins. J. Cell Sci. 114, 161–172.

Tariq, Z., Zhang, H., Chia-Liu, A., Shen, Y., Gete, Y., Xiong, Z.M., Tocheny, C., Campanello, L., Wu, D., Losert, W., Cao, K., 2017. Lamin A and microtubules collaborate to maintain nuclear morphology. Nucleus 8, 433–446.

Thanuja, M.Y., Suma, B.S., Dinesh, D., Ranganath, S.H., Srinivas, S.P., 2021. Microtubule Stabilization Protects Hypothermia-Induced Damage to the Cytoskeleton and Barrier Integrity of the Corneal Endothelial Cells. J. Ocul. Pharmacol. Ther. 37, 399–411.

Thongboonkerd, V., 2019. Proteomics of crystal-cell interactions: A model for kidney stone research. Cells 8, 1076.

Thongboonkerd, V., Semangoen, T., Chutipongtanate, S., 2006. Factors determining types and morphologies of calcium oxalate crystals: Molar concentrations, buffering, pH, stirring and temperature. Clin. Chim. Acta 367, 120–131.

Thongboonkerd, V., Chutipongtanate, S., Semangoen, T., Malasit, P., 2008. Urinary trefoil factor 1 is a novel potent inhibitor of calcium oxalate crystal growth and aggregation. J. Urol. 179, 1615–1619.

Turgay, Y., Eibauer, M., Goldman, A.E., Shimi, T., Khayat, M., Ben-Harush, K., Dubrovsky-Gaupp, A., Sapra, K.T., Goldman, R.D., Medalia, O., 2017. The molecular architecture of lamins in somatic cells. Nature 543, 261–264.

Turgay, Y., Medalia, O., 2017. The structure of lamin filaments in somatic cells as revealed by cryo-electron tomography. Nucleus 8, 475–481.

Uray, I.P., Uray, K., 2021. Mechanotransduction at the Plasma Membrane-Cytoskeleton Interface. Int. J. Mol. Sci. 22, 11566.

Vahabikashi, A., Adam, S.A., Medalia, O., Goldman, R.D., 2022. Nuclear lamins: Structure and function in mechanobiology. APL Bioeng 6, 011503.

van Loosdregt, I., Kamps, M.A.F., Oomens, C.W.J., Loerakker, S., Broers, J.L.V., Bouten, C.V.C., 2017. Lmna knockout mouse embryonic fibroblasts are less contractile than their wild-type counterparts. Integr. Biol. (camb) 9, 709–721.

Vinaiphat, A., Aluksanasuwan, S., Manissorn, J., Sutthimethakorn, S., Thongboonkerd, V., 2017. Response of renal tubular cells to differential types and doses of calcium oxalate crystals: Integrative proteome network analysis and functional investigations. Proteomics 17, 1700192.

Vinaiphat, A., Charngkaew, K., Thongboonkerd, V., 2018. More complete polarization of renal tubular epithelial cells by artificial urine. Cell Death. Discov 5, 47.

Vinaiphat, A., Thongboonkerd, V., 2018. Characterizations of PMCA2-interacting complex and its role as a calcium oxalate crystal-binding protein. Cell. Mol. Life Sci. 75, 1461–1482.

Wang, Y.J., Liang, H., Liu, Y., Bao, Q., Yang, S., Xu, X.X., Chen, Y.C., Liu, W., Shi, X., Shi, Y., Liu, X., Liu, B., Gao, H., Jiu, Y., Liu, Y.J., 2023. Lamin A/C and Vimentin as a Coordinated Regulator during Amoeboid Migration in Microscale Confined Microenvironments. Nano Lett. 23, 6727–6735.

Wuttimongkolchai, N., Kanlaya, R., Nanthawuttiphan, S., Subkod, C., Thongboonkerd, V., 2022. Chlorogenic acid enhances endothelial barrier function and promotes endothelial tube formation: A proteomics approach and functional validation. Biomed. Pharmacother. 153, 113471.

Yoodee, S., Noonin, C., Sueksakit, K., Kanlaya, R., Chaiyarit, S., Peerapen, P., Thongboonkerd, V., 2021. Effects of secretome derived from macrophages exposed to calcium oxalate crystals on renal fibroblast activation. Commun. Biol. 4, 959.

Zhong, Y., Zhang, B., Eum, S.Y., Toborek, M., 2012. HIV-1 Tat triggers nuclear localization of ZO-1 via Rho signaling and cAMP response element-binding protein activation. J. Neurosci. 32, 143–150.